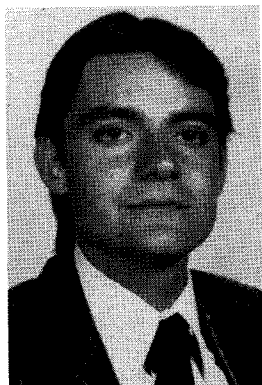
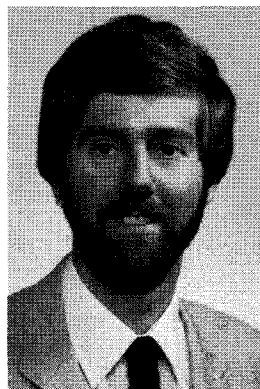


Precast Concrete Connections With Embedded Steel Members



Kostas Marcakis*
Structural Engineer
Read Jones Christoffersen Ltd.
Vancouver
British Columbia



Denis Mitchell
Associate Professor
Department of Civil Engineering
and Applied Mechanics
McGill University
Montreal, Quebec

Connections incorporating embedded structural steel members serving as haunches or brackets have been used for many years in precast concrete construction. Fig. 1 illustrates the application of embedded structural members in a beam-column connection and in a precast panel connection. The advantages of these types of connections are listed below:

(a) In contrast to corbel and headed stud precast connections, the strength of connections with embedded structural steel members is not dependent on the strength of welds.

(b) These types of connections do not usually require complicated reinforcement details.

(c) These connections can be easily designed to exhibit large ductilities.

There are several aspects of embedded steel connections that may require special consideration such as the need to minimize the formation of voids under the embedded member in column connections and the need for fire-proofing for certain applications.

The objective of this paper is to present a rational analytical model and design method for precast concrete connections incorporating embedded steel members. The development of this analytical model is based on the results

*Formerly, Graduate Student, Department of Civil Engineering and Applied Mechanics, McGill University, Montreal, Quebec.

Based on the results of a series of tests on precast concrete connections incorporating embedded steel members, an analytical model capable of predicting the strength of these connections is developed. The predictions using this model and the *PCI Design Handbook* method are compared with the experimental data. A design procedure is proposed and illustrated by two design examples.

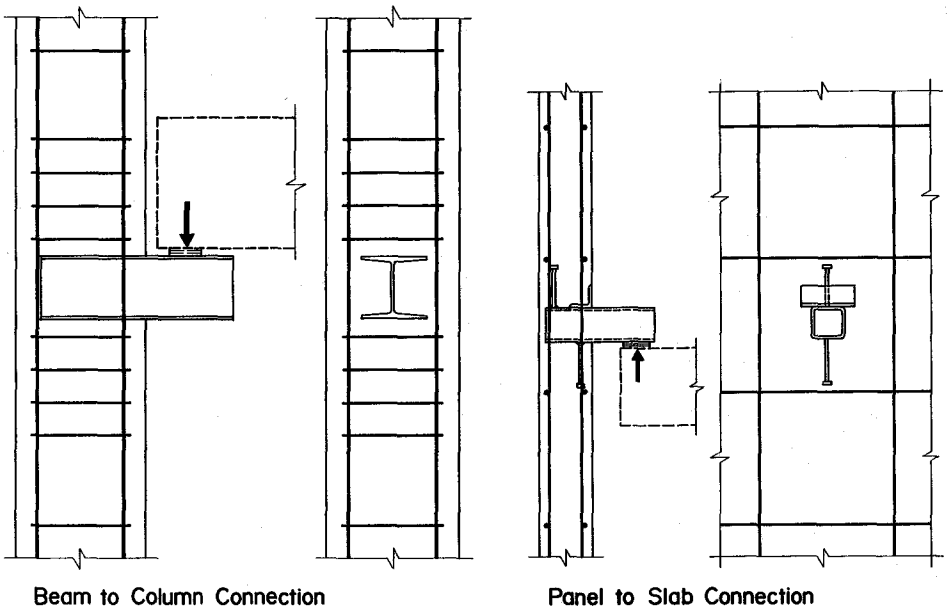


Fig. 1. Precast connections incorporating embedded steel members.

of a series of experiments in which the following variables were studied.

1. Effect of column axial load
2. Effective width of connection
3. Effect of reinforcement welded to connection
4. Effect of shape of embedded member
5. Effect of eccentricity of loading

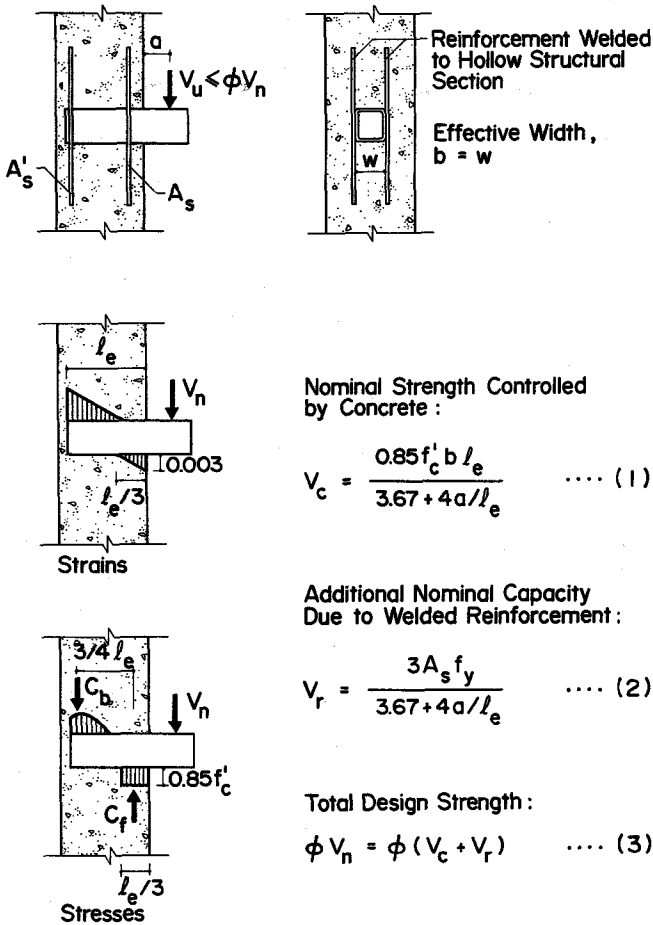


Fig. 2. Equations and assumptions used in designing precast concrete connections with embedded steel members according to *PCI Design Handbook* method (see References 1 through 4).

Current Design Method

The current method for designing precast concrete connections incorporating embedded steel members was first presented in 1971 in the *PCI Design Handbook*.¹ The method was further refined and extended to include the effects of additional welded reinforcement in the Second Edition² of the Handbook. The equations and assumptions (see Fig. 2) on which this

method is based are described in References 3 and 4.

The assumptions of the PCI design method as shown in Fig. 2 are listed below:

1. The effective width of the connection b , is equal to the width of the embedded member, w , and can be increased to $2w$ for double-flanged members provided that the concrete around the section is well compacted and/or confined.

2. The compressive strain at the

front face is assumed to be 0.003 and the depth to the neutral axis is assumed to be $l_e/3$ from the front face of the column.

3. The compressive stress block on the front face at ultimate is assumed to have a depth equal to one-third of the embedment length, l_e .

4. The stress block has a uniform stress of $0.85f'_c$.

5. The resultant compressive force at the back of the embedded member is assumed to be located at $(11/12)l_e$ from the front face of the column.

6. The additional capacity obtained by the presence of welded reinforcement is calculated assuming that the reinforcement acts at the same locations as the concrete stress resultants and that all the welded reinforcement yields at ultimate.

There are several inconsistencies in the assumptions of the PCI design method. For example, the position of the neutral axis depth is assumed to be constant. In reality this depth should vary with the eccentricity of loading and with the amount and location of welded reinforcement. In addition, the assumed neutral axis depth at $l_e/3$ from the front face of the column leads to large strains at the back of the embedded member which is inconsistent with the calculated stress resultant at the back of the member. One cannot assume that the welded reinforcement always yields. This depends on the eccentricity of loading, the amount of reinforcement, the position of reinforcement and the yield stress in the steel. In addition, it is not correct to assume that the reinforcement acts at the same locations as the stress resultants in the concrete.

Experimental Program

A total of 25 precast connections incorporating embedded steel members were tested. The test specimens are

described in Table 1 and are shown in Fig. 3.

Specimens C1, C2, C3, and C4

The first four specimens tested (C1, C2, C3, and C4) comprised a pilot series in order to study the effects of axial load on the connection behavior. All four specimens contained $4 \times 4 \times \frac{1}{4}$ in. (102 x 102 x 6 mm) hollow structural steel members embedded 6 in. (152 mm) into a 7 in. (178 mm) square column. The columns were reinforced with 4—#4 (13 mm diameter) longitudinal bars and 0.28 in. (7 mm) diameter deformed wire ties at 3 in. (76 mm) spacing. The connection load was applied by a hydraulic jack acting through a roller at a distance of 3 in. (76 mm) from the column face. Specimen C1 was tested with zero axial load whereas Specimens C2, C3, and C4 were tested under axial loads of 30, 60, and 90 kips (133, 267, and 400 kN), respectively. The concrete was prevented from entering the hollow structural section during the casting of Specimen C1. The hollow structural sections of Specimens C2, C3, and C4 were filled with concrete over the embedment length.

Specimens SC1, SC2, SC3, SC4, and SC5

The first five specimens of the second series SC1, SC2, SC3, SC4, and SC5 were tested with varying degrees of axial load, i.e., 326, 240, 160, 80, and 0 kips (1450, 1067, 712, 356, and 0 kN), respectively. Specimen SC1 was tested under pure axial load. All five specimens contained a $6 \times 4 \times 0.375$ in. (152 x 102 x 10 mm) hollow structural member embedded 7 in. (178 mm) into a 8 in. (203 mm) square column. The columns were reinforced with 4—#4 (13 mm diameter) longitudinal bars and #3 (10 mm diameter) ties at 3 in. (76 mm) spacing. The hollow structural sections were filled with concrete over the embedment length. Specimen SC2 had an eccentricity of loading of 3 in. (76 mm) from the column face whereas the other specimens had 4 in. (102 mm) eccentricities.

Specimen SC6

Specimen SC6 incorporated a 6×6 in. (152 x 152 mm) wide flange member (W6 x 25) which was modified by cutting

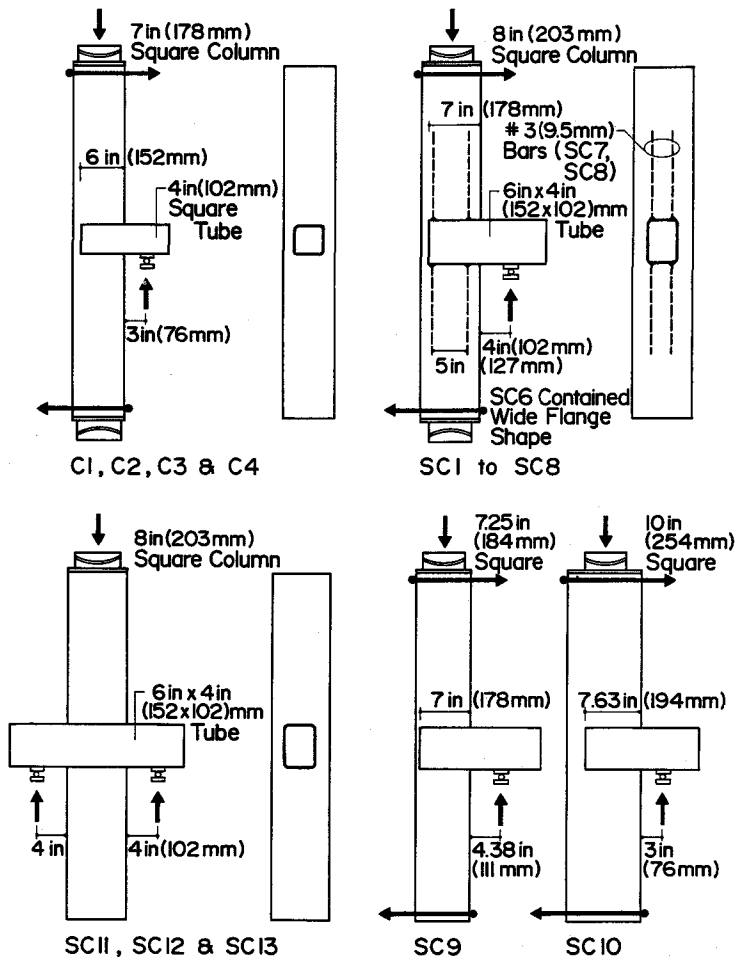


Fig. 3. Details of test specimens.

the flanges such that the width was reduced to 4 in. (102 mm). In all other respects this specimen was identical to Specimen SC5. The purpose of this test was to study the effect of shape of embedded member on the response. The wide flange section was chosen such that when its width was reduced to 4 in. (102 mm) it had approximately the same moment of inertia as the hollow structural section used in Specimen SC5.

Specimens SC7, SC8, and SC14

Specimens SC7 and SC8 had eight 12 in. (305 mm) lengths of #3 (10 mm diameter)

reinforcing bar welded to the embedded member as shown in Fig. 3. These specimens were identical to Specimen SC5 in all other respects. The purpose of these tests was to study the effect of welded reinforcement on the response. Specimen SC14 was identical to Specimens SC7 and SC8 but was tested with a load eccentricity of 8 in. (203 mm) from the column face.

Specimens SC9 and SC10

Specimens SC9 and SC10 had the same column reinforcement as Specimen SC5 but had concrete clear covers of 0.125 in. (3 mm) and 1½ in. (38 mm), respectively.

Table 1. Properties of test specimens.

Specimen	f'_c , psi	f_{er} , in.	a , in.	Column Width, in.	Column Depth, in.	Concrete Cover, in.	Axial Load, kips	Ultimate Shear, kips	Type of Embedded Member	Comments
This investigation										
C1	4800	6	3	7	7	1/2	—	27.8	HSS 4 x 4 x 1/4 in.	HSS not filled
C2	3900	6	3	7	7	1/2	30	41.4	HSS 4 x 4 x 1/4 in.	
C3	5200	6	3	7	7	1/2	60	45.0	HSS 4 x 4 x 1/4 in.	
C4	5800	6	3	7	7	1/2	90	53.5	HSS 4 x 4 x 1/4 in.	
SC1	4500	7	—	8	8	1/2	326	—	HSS 6 x 4 x 3/8 in.	Pure axial load
SC2	4500	7	3	8	8	1/2	240	55.0	HSS 6 x 4 x 3/8 in.	
SC3	4500	7	4	8	8	1/2	160	70.7	HSS 6 x 4 x 3/8 in.	
SC4	4500	7	4	8	8	1/2	80	66.8	HSS 6 x 4 x 3/8 in.	
SC5	4500	7	4	8	8	1/2	—	55.0	HSS 6 x 4 x 3/8 in.	Zero axial load
SC6	4500	7	4	8	8	1/2	—	60.9	W 6 in. x 25 lb/ft.	Flanges cut to 4 in.
SC7	4500	7	4	8	8	1/2	—	80.5	HSS 6 x 4 x 3/8 in.	8 #3 bars welded to HSS
SC8	4500	7	4	8	8	1/2	—	83.5	HSS 6 x 4 x 3/8 in.	8 #3 bars welded to HSS
SC9	4500	7	4 3/8	7 1/4	7 1/4	1/8	—	49.1	HSS 6 x 4 x 3/8 in.	1/8 in. cover
SC10	4500	7 3/8	3	10	10	1 1/2	—	62.8	HSS 6 x 4 x 3/8 in.	1 1/2 in. cover
SC11	4500	8	4	8	8	1/2	—	220.0	HSS 6 x 4 x 3/8 in.	"Pure shear"
SC12	4500	8	4	8	8	1/2	—	212.0	W 6 in. x 25 lb/ft.	"Pure shear"
SC13	4500	8	4	8	8	1/2	—	210.0	HSS 6 x 4 x 3/8 in.	"Pure shear"
SC14	4800	7	8	8	8	1/2	—	47.6	HSS 6 x 4 x 3/8 in.	8 #3 bars welded to HSS
TC1	3400	7 1/4	4	16	8	1/2	—	58.9	4 in. square steel bar	Very wide column
TC2	3400	7 1/4	4	8	8	1/2	—	32.3	4 in. square steel bar	Reduced width at connection
TC3	3400	8	4	8	8	1/2	—	17.5	4 in. square steel bar	Reduced width; pure moment
TC4	3400	8	4	8	8	1/2	—	26.0	HSS 6 x 4 x 3/8 in.	Pure moment
PL1	6900	4	3	8.0	5.0	3/8	—	19.6	3/4 x 4 in. plate	Embedded plate connection
PL2	6900	4	3	8.0	5.0	3/8	—	31.1	3/4 x 4 in. plate	4 in. angle welded to plate
PL3	6900	4	3	8.0	5.0	3/8	—	42.8	3/4 x 4 in. plate	Angle and reinforcing bars welded to plate
Tests by Clarke and Symmons (Reference 6). Note: f'_c assumed to be 0.8 x cube strength										
D1(1)	3840	4.9	2	5.9	5.9	0.4	33.7	18.0	1 1/2 in. square billet	
D1(2)	3840	4.9	2	5.9	5.9	0.4	33.7	18.0	1 1/2 in. square billet	
D1(3)	3840	4.9	2	5.9	5.9	0.4	33.7	18.0	1 in. square billet	
D2(1)	3020	4.9	2	5.9	5.9	0.4	33.7	18.9	2 in. square billet	
D2(2)	2410	4.9	2	5.9	5.9	0.4	33.7	16.0	2 in. square billet	
D2(3)	2410	4.9	2	5.9	5.9	0.4	33.7	16.6	2 in. square billet	
D3(1)	3130	4.9	2	5.9	5.9	0.4	33.7	20.9	2 x 1 1/2 in. billet	
D3(2)	3130	4.9	2	5.9	5.9	0.4	33.7	21.8	2 x 1 1/2 in. billet	
D3(3)	3130	4.9	2	5.9	5.9	0.4	33.7	21.1	2 x 1 1/2 in. billet	
D4(1)	3860	4.9	2	5.9	5.9	0.4	33.7	29.2	3 x 2 in. billet	

NOTE: 1 in. = 25.4 mm; 1 kip = 4.448 kN; 1 ksi = 6.895 MPa.

cast building. Specimen SC12 incorporated the same wide flange section as used in Specimen SC6 and was identical to Specimens SC11 and SC13 in all other respects. The purpose of this test was to study the effect of shape of embedded member on the behavior.

Specimen TC1

Specimen TC1 had a column which was

16 in. (406 mm) wide x 8 in. (203 mm) deep and was reinforced with 4—#8 (25 mm diameter) bars and #3 (10 mm) ties at 3 in. (76 mm) spacing. This specimen contained a 4 in. (102 mm) square solid steel member with an embedment length of 7.25 in. (184 mm) and a load applied 4 in. (102 mm) from the column face. The objective of this test was to study the effect of column width on the response.

Specimens TC2 and TC3

In each of Specimens TC2 and TC3 two styrofoam blocks 8 x 8 x 2 in. (203 x 203 x 51 mm) thick were cast in the column adjacent to the steel member. This resulted in a reduced 4 in. (102 mm) width of concrete above and below the embedded member (see Fig. 3). Outside of the connection region the column was 8 in. (203 mm) square and was reinforced with 4-#5 (16 mm diameter) longitudinal bars with #3 (10 mm) ties at 3 in. (76 mm) spacing. The embedded member in both specimens consisted of a 4 in. (102 mm) square solid steel bar. Specimen TC2 had the same embedment length and loading as Specimen TC1. The purpose of Specimen TC2 was to study the strain distribution in the concrete above and below the connection. The embedded member in Specimen TC3 protruded from both faces of the column. Two equal and opposite loads were applied with equal eccentricities as shown in Fig. 3. The purpose of this test was to study the response of a specimen with reduced column width under a "pure moment" loading. Although this antisymmetrical loading condition is unusual it was useful in the development of the analytical model. Since Specimens TC2 and TC3 had reduced widths in the connection region exposing the sides of the embedded member it was possible to measure strains in the concrete along the embedment length.

Specimen TC4

Specimen TC4 was identical to Specimens SC11 and SC13 except that it was tested under "pure moment" loading as shown for Specimen TC3.

Specimens PL1, PL2, and PL3

Three specimens (PL1, PL2, and PL3) were tested to study the behavior of precast panel connections using embedded steel plates. In all three specimens the panel was represented by an 8 x 5 in. (203 x 127 mm) column reinforced with 4-#5 vertical bars and #3 ties at 3 in. (76 mm) spacing. Specimen PL1 contained a 3/4 in. thick x 4 in. deep (19 x 102 mm) plate embedded 4 in. (102 mm) into the panel. The plate was loaded 3 in. (76 mm) from the panel face. Specimen PL2 was identi-

Table 2. Properties of reinforcing bars.

Bar size designation	Diameter, in.	Area, in. ²	Yield strength, ksi
D6	0.276	0.06	80.0
#3	0.375	0.11	73.0
#4	0.500	0.20	48.9
#5	0.625	0.31	60.3
#8	1.000	0.79	59.5

NOTE: 1 in. = 25.4 mm; 1 in.² = 645 mm²; 1 ksi = 6.895 MPa.

cal to Specimen PL1 but in addition contained a 4 in. (102 mm) long 2 in. x 2 in. x 1/4 in. (51 x 51 x 6 mm) angle welded to the steel plate as shown in Fig. 3. The purpose of this test was to study ways of improving the bearing of embedded plates in precast panels. Specimen PL3 contained reinforcement and an angle welded to the plate as shown in Fig. 3. The reinforcement consisted of 2-#3 (10 mm) reinforcing bars welded close to the front face (one bar on each side of the plate) and 1-#4 (13 mm) reinforcing bar welded along the end of the plate. The purpose of this experiment was to study the effect of reinforcement on the response.

Material Properties

The concrete strengths at the time of testing are given in Table 1. The properties of the reinforcing bars used are given in Table 2. The hollow structural sections used had a specified minimum yield stress of 50 ksi (345 MPa). The 4 in. (102 mm) square solid steel member had a minimum yield stress of 47 ksi (324 MPa). The plates, angles and wide flange members used had a minimum specified yield stress of 44 ksi (303 MPa).

Instrumentation

Deflection of the embedded member relative to the column at the point of application of the load was measured by dial gauges to the nearest 0.001 in. (0.025 mm). Strains were measured in the vertical column reinforcement in the region of the connection. Concrete strains were measured on the front face of each column with more extensive strain measurements taken on Specimens C1, TC2, and TC3. More details can be found in Reference 5.

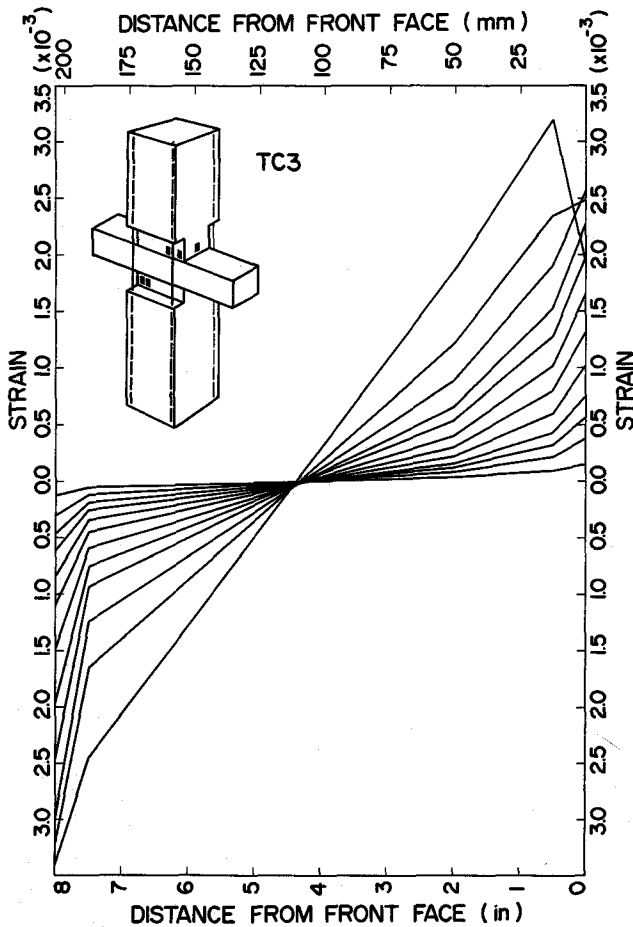


Fig. 4a. Measured strain distributions from front face of Specimen TC3.

Analytical Model

An attempt is made to develop a rational analytical model capable of predicting the ultimate capacity of a variety of embedded steel member precast connections.

Strain Distribution at Ultimate

Specimens TC2 and TC3 were specially constructed to enable measurements of concrete strain along the embedment length (see Figs. 4a and 4b). Specimen TC3 was subjected to "pure

moment" loading and as expected the measured strains indicate a reasonably symmetrical and linear strain distribution. The maximum strain recorded at the surface of the column was 0.0034. Specimen TC2 was eccentrically loaded and indicated a relatively linear strain distribution with a maximum measured strain at the front face of the column of 0.0038. The neutral axis was located at a distance of 5.25 in. (133 mm) from the front face of the column. Due to a splitting crack through one strain gauge no readings were possible at the back of

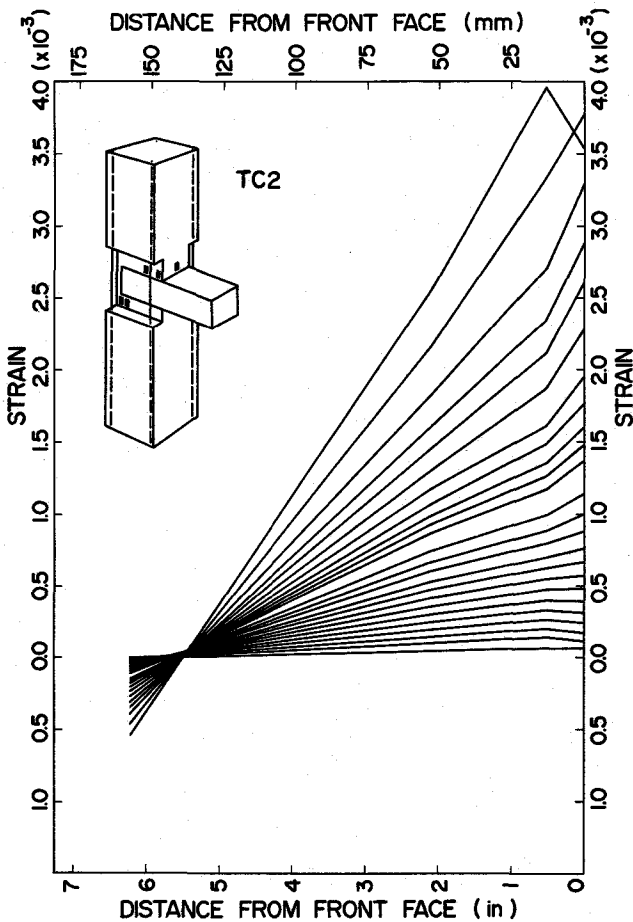


Fig. 4b. Measured strain distributions from front face of Specimen TC2.

the embedded member. From these measurements and to conform with existing assumptions a linear strain distribution with a maximum strain at the front face of 0.003 will be assumed. In addition, in calculating the stress resultant at the front face the ACI stress block factors will be used.

Equilibrium

The position of the neutral axis is not constant but will depend on the eccentricity of loading. The above assumptions result in a uniform strain distribution of 0.003 for the "pure

shear" case of loading with a resulting uniform stress distribution of $0.85 f'_c$ as shown in Fig. 5a. The pure moment loading case results in an antisymmetrical strain distribution with the neutral axis located at the center of the embedment length, l_e . Since the maximum concrete strains are assumed to be 0.003 at both column faces, this results in a uniform stress block with a magnitude of $0.85 f'_c$ and a depth of $\beta_1 l_e / 2$ from each column face as shown in Fig. 5b. Tensile stresses in the concrete are neglected.

The more general loading condition

is shown in Fig. 5c and results from either an embedded member protruding from one side or a two-sided connection with unbalanced loading (see Design Example 2). A front face strain, ϵ_f , of 0.003 is assumed with a linear strain distribution. However, the depth of the neutral axis x_f is unknown. In order to find x_f , conditions of equilibrium must be applied. The ACI stress block factors are used to calculate the stress resultant, C_f , near the front. For this loading the strain at the back of the embedded member, ϵ_b , is less than 0.003. In order to find the magnitude and position of the stress resultant near the back of the embedded member, it is necessary to define the stress-strain relationship for the concrete in compression. The parabolic stress-strain relationship assumed is given below:

$$f_c = f'_c \left[2 \frac{\epsilon_c}{\epsilon_o} - \left(\frac{\epsilon_c}{\epsilon_o} \right)^2 \right] \quad (4)^*$$

*Note that Eqs. (1), (2), and (3) are given in Fig. 2.

where

- f'_c = concrete compressive strength
- ϵ_c = concrete strain
- f_c = concrete stress corresponding to ϵ_c
- ϵ_o = strain at maximum concrete stress assumed to be 0.002 (short-term concrete cylinder tests indicate a strain of approximately 0.002 when $f_c = f'_c$).

In calculating the stress resultant near the back of the connection, it is convenient to replace the parabolic stress distribution with an equivalent uniform stress distribution having a uniform stress $\alpha f'_c$ and acting over a depth of βx_b , where x_b is the depth of the strain distribution from the back of the connection (see Fig. 5c).

The values of the coefficients α and β will depend on the shape of the assumed stress distribution and on the strain at the back of the connection, ϵ_b . These values of α and β have been determined such that the magnitude and position of the resulting uniform

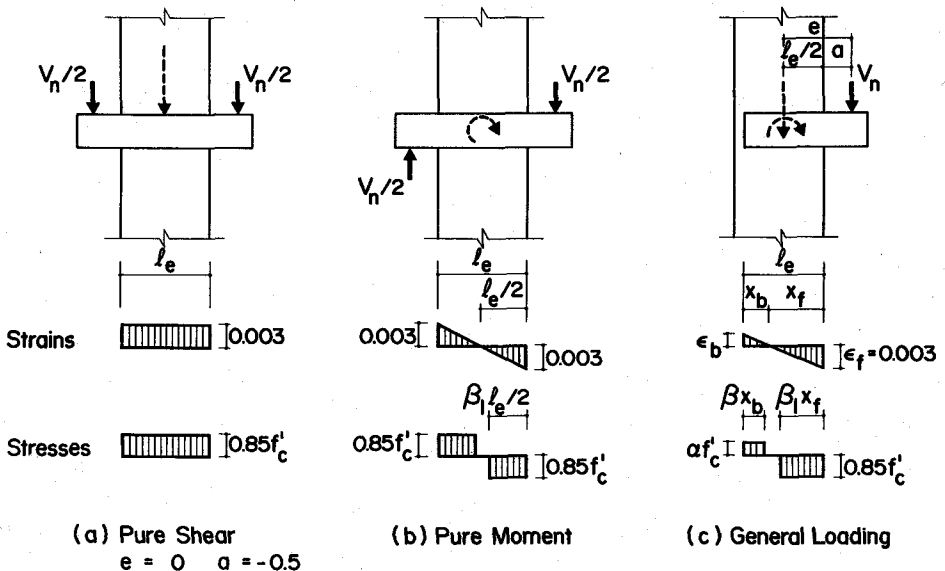
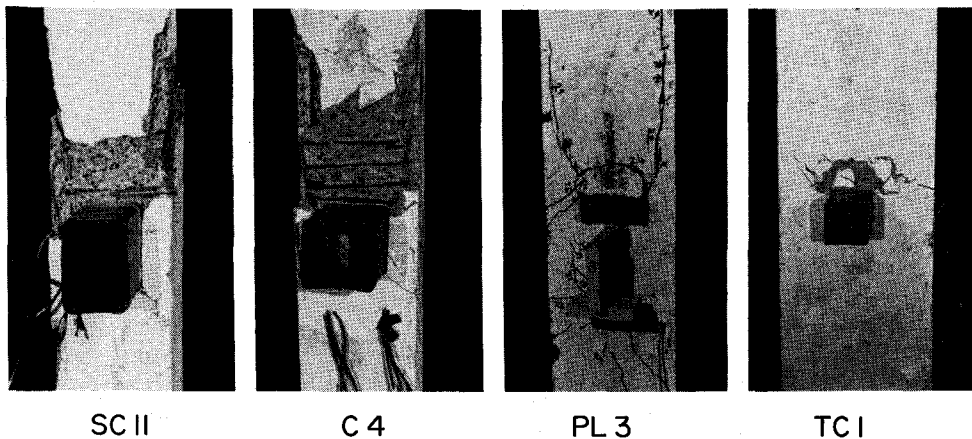


Fig. 5. Strain and stress distribution for pure shear, pure moment and general loading.



SC II "Pure Shear" Test C 4 Spalling of Concrete Cover PL 3 Steel Angle Used to Increase Effective Width TC I Wide Specimen

Fig. 6. Load spreading in various tests (Specimens SC11, C4, PL3, and TC1).

stress distribution are the same as those for the parabolic stress distribution. The resulting stress block factors corresponding to ϵ_b are:

$$\alpha\beta = \frac{\epsilon_b}{\epsilon_o} - \frac{1}{3} \left(\frac{\epsilon_b}{\epsilon_o} \right)^2 \quad (5)$$

and

$$\beta = \frac{4 - \frac{\epsilon_b}{\epsilon_o}}{6 - 2 \frac{\epsilon_b}{\epsilon_o}} \quad (6)$$

The resulting equilibrium conditions for the connection at ultimate can be expressed as:

$$V_n = 0.85f'_c b \beta_1 x_f - \alpha f'_c b \beta x_b \quad (7)$$

where

V_n = resultant of the vertical loads acting on the connection at ultimate

b = effective width of the connection

β_1 = ACI stress block factor

x_b = depth of the strain distribution from the back of the connection ($x_f + x_b = l_e$)

Taking moments about the front face of the column gives:

$$V_n a = (\alpha f'_c b \beta x_b) (l_e - \beta x_b / 2) - 0.85 f'_c b \beta_1 x_f (\beta_1 x_f / 2) \quad (8)$$

where

a = distance from the front face of the connection to the resultant of the vertical loads and is positive for resultant shear forces outside the column and negative for resultant forces inside the column.

For a given loading configuration the two unknowns, V_n and x_f , can be found from Eqs. (7) and (8) and thus the capacity of the connection is determined.

Effective Width (see Fig. 6)

The ultimate strength predictions of the test specimens using Eqs. (7) and (8) with an effective width equal to the width of the embedded member

are overly conservative. Due to the confinement of the concrete in the connection region, the load is able to spread to a width greater than the width of the embedded member. This confinement results in stresses greater than the unconfined compressive strength immediately adjacent to the embedded member. The four specimens shown in Fig. 6 illustrate the ability of the load to spread. Specimen SC11 was a pure shear test (see Fig. 5) and therefore a uniform stress distribution of $0.85f'_c$ was assumed.

A comparison of the calculated capacity with the measured strength indicates that the effective width for this connection is equal to the width of the concrete confined by the column ties measured to the outside of the ties. This phenomenon is illustrated in the photograph of Specimen C4 in Fig. 6 in which spalling of the concrete cover occurred to the outside of the confining ties indicating load spreading to this effective width.

The photograph of Specimen PL3 illustrates a method of increasing the effective width by including an angle welded to the embedded plate member. Specimen TC1 was tested in order to study the limits of spreading in wide specimens. As can be seen from Fig. 6 the spreading was not able to extend to the outside of the ties but was limited in width. Measurement of the spalling width together with a comparison of calculated capacity with measured strength indicate an effective width approximately equal to 3.2 times the width of the embedded member for Specimen TC1.

In predicting the capacity of these types of connections, an effective width equal to the width of the confined region will be assumed. For specimens whose width is large compared to the width of the embedded member and in the presence of confining reinforcement, a maximum effective width of 2.5 times the width of

the embedded member will be assumed. This limit on the effective width was chosen in order that the prediction of capacity for wide specimens would provide approximately the same safety margin as for the other specimens.

Analysis of Connections with Additional Reinforcement

In predicting the strength of connections containing additional reinforcement welded to the embedded member, it is assumed that the steel reinforcement can act in tension or compression and that the strain in the steel is equal in magnitude to the compressive strain in the concrete at the same location as the steel. In order to enable the reinforcement to reach yield, proper development length must be provided. The equilibrium conditions for connections with welded reinforcement are:

$$V_n = 0.85f'_c b \beta_1 x_f + A_s f_s - \alpha f'_c b \beta x_b - A'_s f'_s \quad (9)$$

$$V_n a = (\alpha f'_c b \beta x_b) \left(l_e - \frac{\beta x_b}{2} \right) + A'_s f'_s d_b - 0.85f'_c b \beta_1 x_f (\beta_1 x_f / 2) - A_s f_s d_f \quad (10)$$

where

- V_n = resultant of vertical loads acting on connection
- A_s, A'_s = total effective area of welded reinforcement near front and back, respectively
- f_s, f'_s = steel stress in welded reinforcement near front and back, respectively
- d_f = distance from front face to center of reinforcement near front
- d_b = distance from front face to center of reinforcement near back

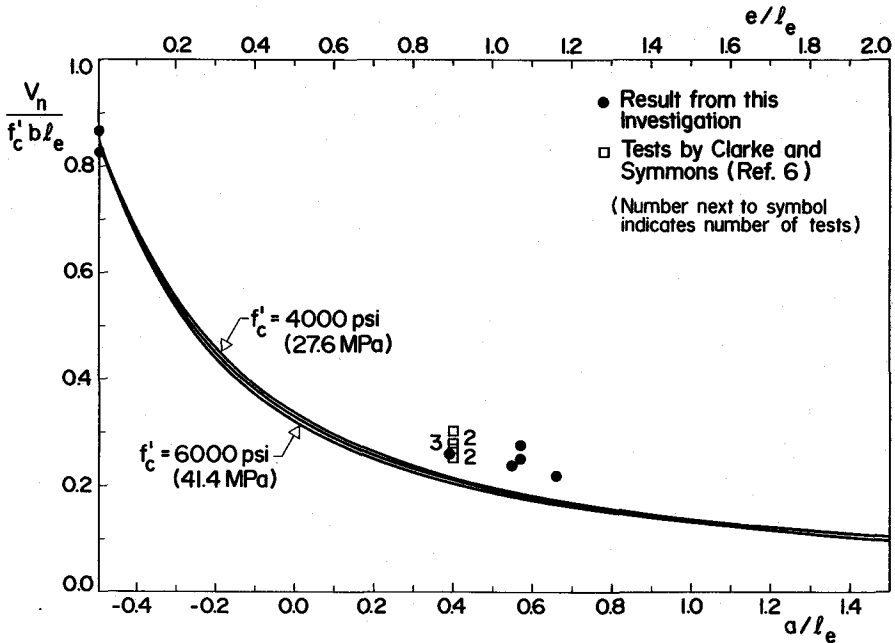


Fig. 7. Comparison of predictions with test results (connections without additional reinforcement). Data points are shown of test results from this investigation and those by Clarke and Symmons.⁶

The steel stresses f_s and f'_s can be calculated as:

$$f_s = 0.003 E_s [1 - d_f/x_f] \leq f_y \quad (11)$$

$$f'_s = 0.003 E_s [d_b/x_f - 1] \leq f_y \quad (12)$$

For a given connection with welded reinforcement the two unknowns, V_n and x_f , can be found by solving Eqs. (9) and (10).

Prediction of Test Results

Although Eqs. (7) and (8) can be solved for specific connection details and material properties, it is more useful to solve them in a general manner. The solution technique used involves choosing a value of the neutral axis depth, x_f , which defines the strain distribution and enables stress resultants to be calculated. The equilibrium conditions can then be applied to solve for the non-dimension-

alized connection strength, $V_n/(f'_c b l_e)$, and the non-dimensionalized position of the loading resultant, a/l_e . If this procedure is repeated for a range of values of x_f , then the graph shown in Fig. 7 can be produced.

Another useful way of describing the eccentricity of loading is the distance from the center of embedment to the position of the resultant of applied loads, e (where $e = a + l_e/2$). As can be seen from Fig. 7 the maximum connection strength is obtained under a "pure shear" loading condition in which $e = 0$ or $a/l_e = -0.5$. As the eccentricity of loading is increased, the capacity of the connection decreases. Fig. 7 compares the results of experiments from Reference 6 and from this investigation with the predicted values. As can be seen, the analytical model conservatively predicts the capacities.

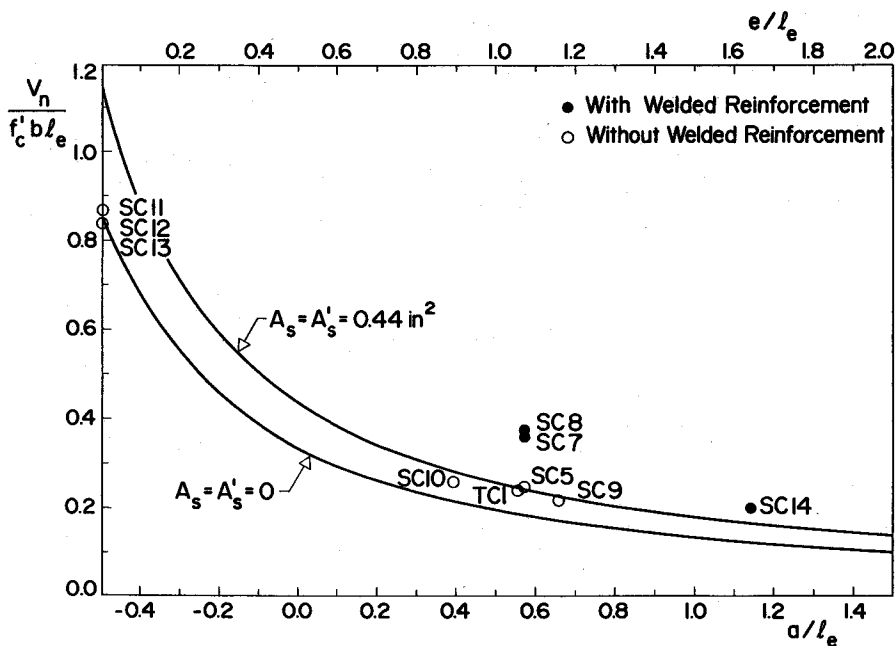


Fig. 8. Comparison of predictions with test results (connections with and without additional reinforcement).

Fig. 8 was obtained by applying a similar solution technique to Eqs. (9) and (10). The strength predictions depend on the yield stress of the reinforcement and the position of the reinforcement and thus these variables were made equal to the experimental values. As can be seen from Fig. 8, the analytical model conservatively predicts the increase in capacity due to the presence of welded reinforcement.

Table 3 compares both the predictions of the analytical model and the *PCI Design Handbook* method with test results from this investigation and Reference 6. (Note that the specimens are described in Table 1.) As can be seen from Table 3, the analytical model conservatively predicts the capacity of all the test results except for Specimen C1 in which local bending occurred in the hollow structural section. It is noted that

Specimens C2, C3, C4, SC2, SC3, SC4, and the D series from Reference 6 had axial loads acting on the columns. It is apparent that the PCI method is very conservative.

Effects of Additional Welded Reinforcement

Fig. 9 compares the load-deflection responses of Specimen SC5 (without additional welded reinforcement) with Specimen SC8 (with additional welded reinforcement). As can be seen, the presence of welded reinforcement greatly increases the capacity and the stiffness of the connection. Both specimens failed in the concrete exhibiting deflections at a maximum load of 0.152 and 0.199 in. (4 and 5 mm) for Specimens SC5 and SC8, respectively. The analytical model predicts an increase of 34 percent due to the presence of welded reinforcement. Specimen SC8 had a

Table 3. Comparison of analytical model and PCI method with test results.

Specimen	<i>b</i> , in.	V_{exp} , kips	V_{PCI} , kips	V_n , kips	$\frac{V_{exp}}{V_{PCI}}$	$\frac{V_{exp}}{V_n}$	Comments	
This Investigation								
C1	6.0	27.8	18.9	33.3	1.48	0.83	Local bending of thin wall	
C2	6.0	41.4	14.0	27.3	2.96	1.52		
C3	6.0	45.0	18.7	35.7	2.41	1.26		
C4	6.0	53.5	20.9	39.4	2.56	1.36		
SC2	7.0	55.8	19.9	45.1	2.80	1.24		
SC3	7.0	70.7	18.0	40.0	3.93	1.77		
SC4	7.0	66.8	18.0	40.0	3.71	1.67		
SC5	7.0	55.0	18.0	40.0	3.06	1.38		
SC6	7.0	60.9	18.0	40.0	3.38	1.52		Wide flange member
SC7	7.0	80.5	31.4	52.7	2.56	1.53		
SC8	7.0	83.5	31.4	52.7	2.66	1.58		Reinforced
SC9	7.0	49.1	17.3	38.5	2.84	1.28		
SC10	7.0	62.8	20.3	45.6	3.09	1.38		
SC11	7.0	220.0	81.6	214.2	2.70	1.02		Pure shear
SC12	7.0	212.0	81.6	214.2	2.60	.99	Pure shear	
SC13	7.0	210.0	81.6	214.2	2.57	.98	Pure shear	
SC14	7.0	47.6	13.9	32.2	3.42	1.48	Reinforced	
TC1	10.0	58.9	14.3	46.2	4.12	1.27	Wide specimen	
PL1	1.9	19.6	2.6	8.4	7.54	2.33	Embedded plate	
PL2	4.5*	31.1	14.1	20.0	2.21	1.56	Plate with angle	
PL3	4.5*	42.8	20.7	24.8	2.07	1.73	Plate with angle and reinforcement	
Tests by Clarke and Symmons† (Reference 6). All specimens had 33.7 kips axial load.								
D1(1)	3.75	18.0	4.5	14.8	4.00	1.21		
D1(2)	3.75	18.0	4.5	14.8	4.00	1.21		
D1(3)	3.75	18.0	4.5	14.8	4.00	1.21		
D2(1)	5.00	18.9	4.7	15.7	4.00	1.20		
D2(2)	5.00	16.0	3.8	12.6	4.18	1.27		
D2(3)	5.00	16.6	3.8	12.6	4.35	1.32		
D3(1)	5.00	20.9	4.9	16.2	4.23	1.29		
D3(2)	5.00	21.8	4.9	16.2	4.41	1.35		
D3(3)	5.00	21.1	4.9	16.2	4.27	1.31		
D4(1)	5.12	29.2	9.2	25.4	3.17	1.15		

*An average of the front and back effective widths was used.

†Other tests from Reference 6 did not contain column ties

NOTE: 1 in. = 25.4 mm; 1 kip = 4.448 kN.

52 percent larger capacity than Specimen SC5. This large increase may be due to strain hardening in the reinforcement.

Effects of Type of Embedded Member

Fig. 10 compares the load-deflection responses of Specimen SC5 containing a hollow structural steel embedded member with Specimen SC6

incorporating a wide flange embedded member. The load-deflection responses indicate that the specimen containing the wide flange embedded member is stiffer and has an 11 percent higher capacity than the specimen with the hollow structural steel section. Specimens SC5 and SC6 exhibited deflections at ultimate of 0.152 and 0.131 in. (4 and 3 mm), respectively.

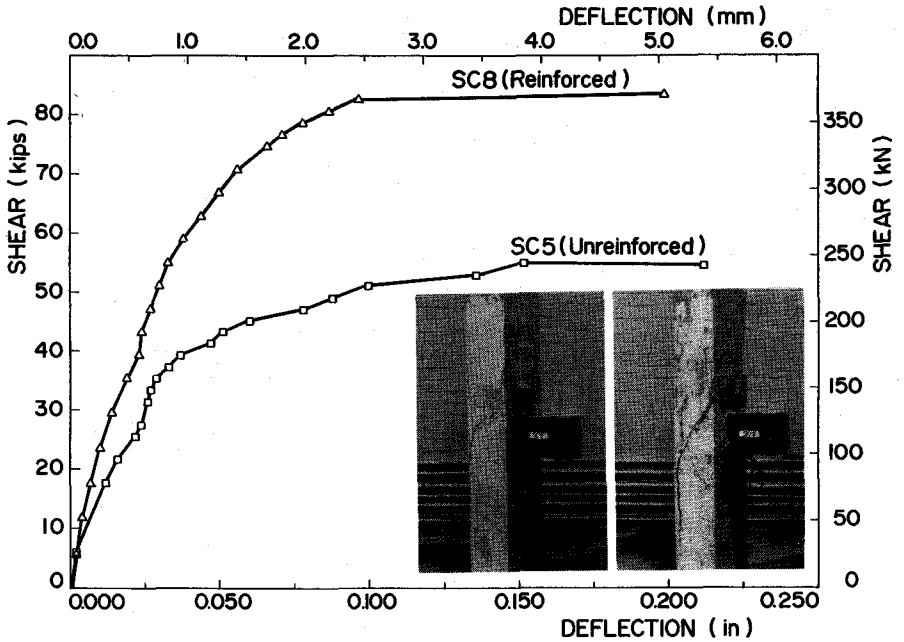


Fig. 9. Effect of additional welded reinforcement on response.

An examination of the photographs of these two specimens at failure indicates that inclined vertical cracks are formed from both the top and bottom flanges of the wide flange section. This indicates that both flanges are effective in distributing the load. The hollow structural steel member, on the other hand, has only one loading surface to distribute the load. Therefore, a wide flange section results in a more favorable distribution of stresses in the connection.

Specimen PL1 contained a $\frac{3}{4}$ in. (19 mm) thick plate embedded in a precast panel. A comparison of the analytical prediction with the experimental results indicates that the effective width for this specimen is approximately five times the width of the plate. This demonstrates the high degree of confinement possible for this type of connection. Specimen PL2 contained a 4 in. (102 mm) long angle welded to the $\frac{3}{4}$ in. (19 mm)

plate (see Fig. 3). As can be seen from Fig. 6 the presence of this angle greatly increased the effective width of the connection. Load spreading was observed to extend to the width of the region confined by ties.

Specimen C1 incorporated a 4 x 4 x 0.25 in. (102 x 102 x 6 mm) hollow structural section that was not filled with concrete along its embedment length.

Since the hollow structural steel member had thin walls and since it was not filled with concrete, the bearing of the concrete against the top wall of the steel member caused severe local bending. This resulted in stress concentrations in the concrete above the webs of the hollow steel member, which reduced the effective width of the connection and led to a premature failure. Therefore, if the walls of a hollow structural steel member are not stiff enough, it should be filled with concrete to ensure a

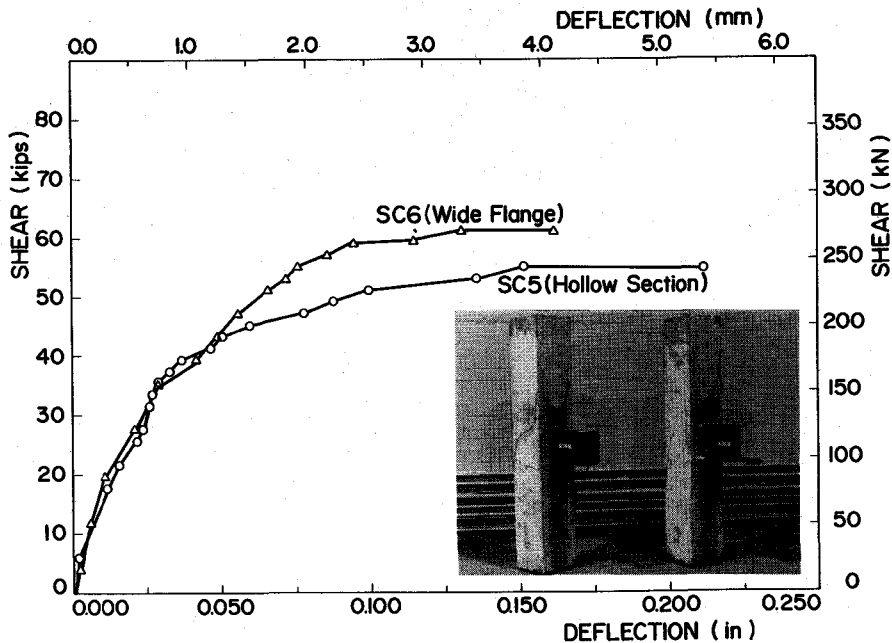


Fig. 10. Effect of shape of embedded member on response.

more uniform bearing stress which will enable the effective width to attain its maximum value.

More research is required to quantify the effects of various types of embedded members on the response. Therefore, in applying the analytical model the beneficial effects attributed to shape (e.g., a wide flange section) are neglected.

Effects of Column Axial Load

The load-deflection responses of four identical specimens (SC2, SC3, SC4, and SC5) with various levels of column axial load are shown in Fig. 11a. In addition, Specimen SC1 was tested under pure axial load and failed at a load of 326 kips (1450 kN). As can be seen from Fig. 11a, as the level of axial load was increased, the deflection at ultimate, which is a measure of ductility, decreased.

Fig. 11b shows the axial load-shear interaction diagram for the five

specimens tested, where P is the axial load on the column during the test and P_o is the pure axial load capacity of the column. As can be seen from the interaction diagram the shear capacity of the connection increases with increasing axial load until a maximum shear capacity is reached when the column is subjected to approximately 50 percent of its axial capacity.

For values of axial load greater than 50 percent of the axial capacity of the column the shear capacity decreases with increasing axial load. The shear capacities of the connection for axial loads less than 75 percent of the axial capacity of the column were greater than the capacity of the connection at zero axial load.

The analytical model can therefore be used to conservatively predict the capacity of connections where the axial load in the column does not exceed 75 percent of its axial capacity.

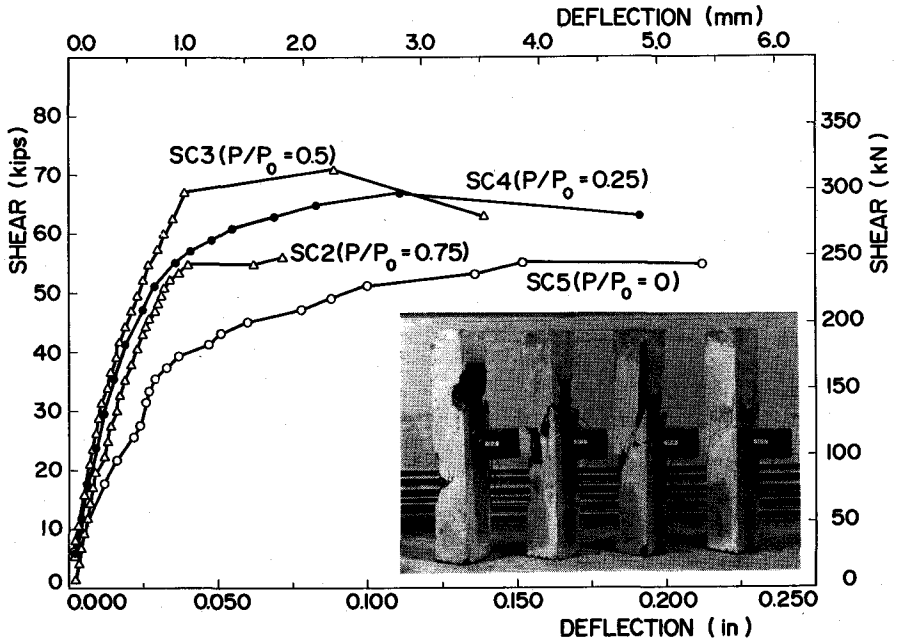


Fig. 11a. Effects of axial load on response (Specimens SC2, SC3, SC4, and SC5).

The photographs in Fig. 11a illustrate the increased spalling that occurs as the axial load level is increased. In addition, the diagonal cracks on the sides of the column become steeper as the axial load is increased.

Proposed Design Method

In order to facilitate the design of embedded structural member precast connections the design curves shown in Fig. 12 are presented. In the preparation of these curves it was assumed that there was an equal amount of reinforcement welded to the front and the back of the embedded member (i.e., $A_s = A'_s$). It was also assumed that the steel reinforcement was placed symmetrically about the center of embedment.

The amount of reinforcement is expressed in terms of a reinforcement index ω , where:

$$\omega = \frac{A_s}{bl_e} \cdot \frac{f_y}{f'_c}$$

The position of the reinforcing steel is expressed in terms of the ratio s/l_e , where s is the distance between symmetrically placed A_s and A'_s . In many cases the welded reinforcement will not be symmetrically placed about the center of embedment. For these cases it was found that the use of a spacing, s , equal to twice the distance from the center of embedment to the nearest welded reinforcement yielded conservative predictions.

The design curves in Fig. 12 were prepared for f'_c less than or equal to 4000 psi (27.6 MPa). It can be seen from Fig. 7 that the non-dimensionalized capacity, $V_n/(f'_c bl_e)$, is only slightly affected by the value of f'_c (due to the dependance of β_1 on f'_c). Since the analytical model is conservative, this effect may be neglected.

These curves may be used to design

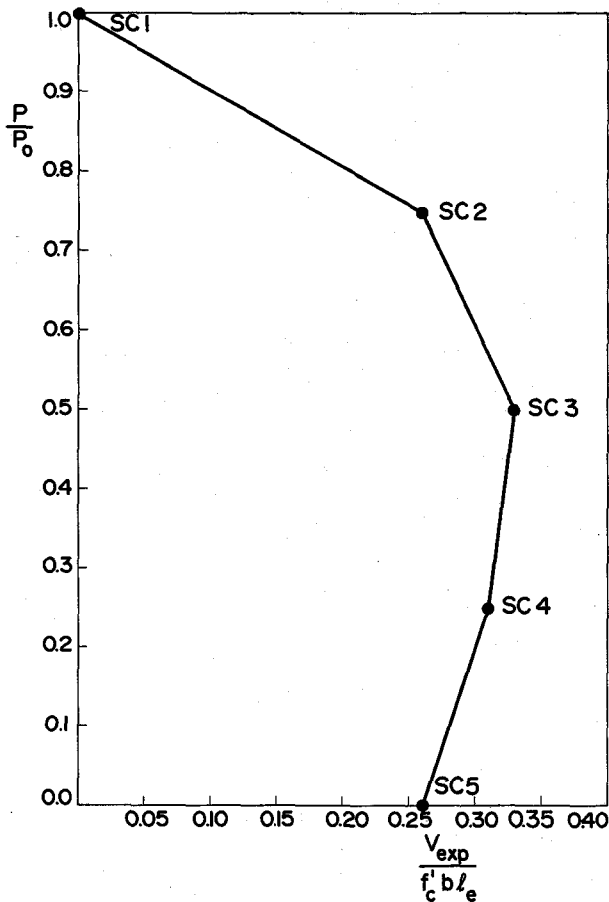


Fig. 11b. Axial load versus shear interaction diagram (Specimens SC1, SC2, SC3, SC4, and SC5).

or to analyze a connection. In design, the material properties and the column or panel dimensions are usually known and the designer would choose suitable values of embedment length, l_e , eccentricity of load from the front face, a , and width of embedded member, w . An effective width, b , is chosen based on the column details and the width of embedded member, w (note that $b \leq 2.5 w$).

The designer would then be able to enter the appropriate design curve of Fig. 12 with a/l_e and $V_u/(\phi f'_c b l_e)$

(where V_u is the design shear) and thus determine if the connection requires reinforcement. If reinforcement is required the designer can choose an arrangement of reinforcement and then use linear interpolation to find the required ω corresponding to the value of s/l_e .

As can be seen from Fig. 12, the nominal strength of a connection is a function of the eccentricity, e/l_e , the spacing of the reinforcement, s/l_e , and the amount of reinforcement, ω . In order to facilitate design, simplified

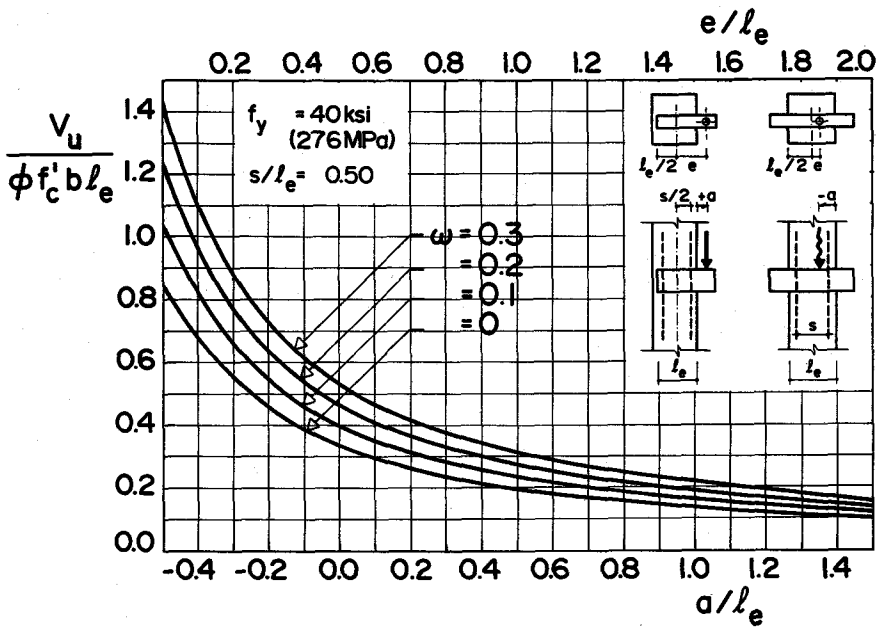


Fig. 12a. Design chart for evaluating parameters ($f_y = 40 \text{ ksi}$, $s/l_e = 0.50$).

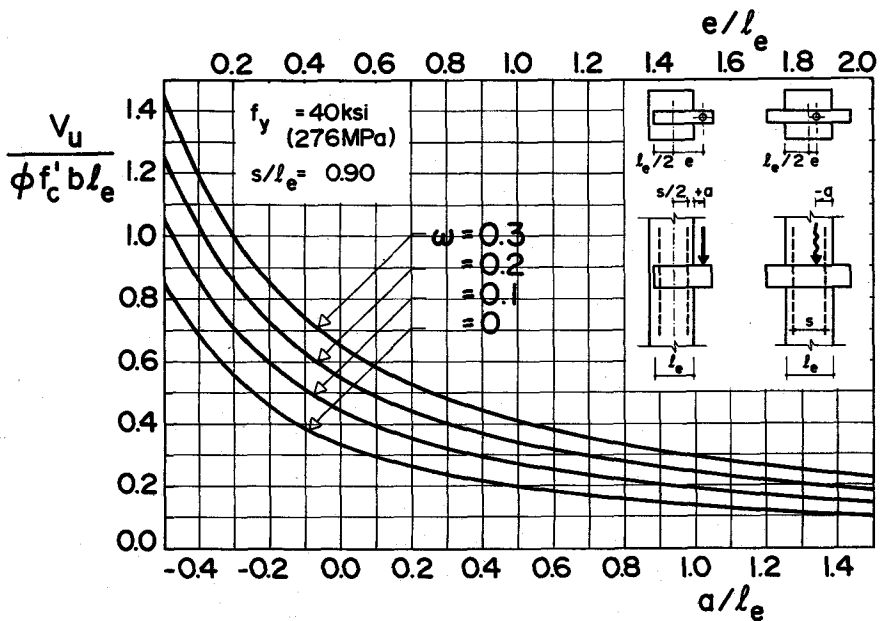


Fig. 12b. Design chart for evaluating parameters ($f_y = 40 \text{ ksi}$, $s/l_e = 0.90$).

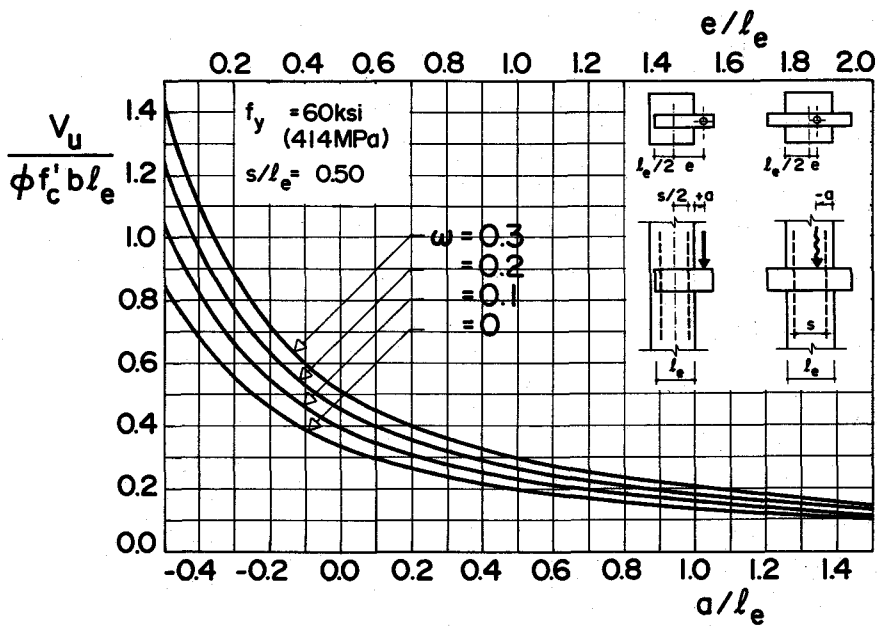


Fig. 12c. Design chart for evaluating parameters ($f_y = 60 \text{ ksi}$, $s/l_e = 0.50$).

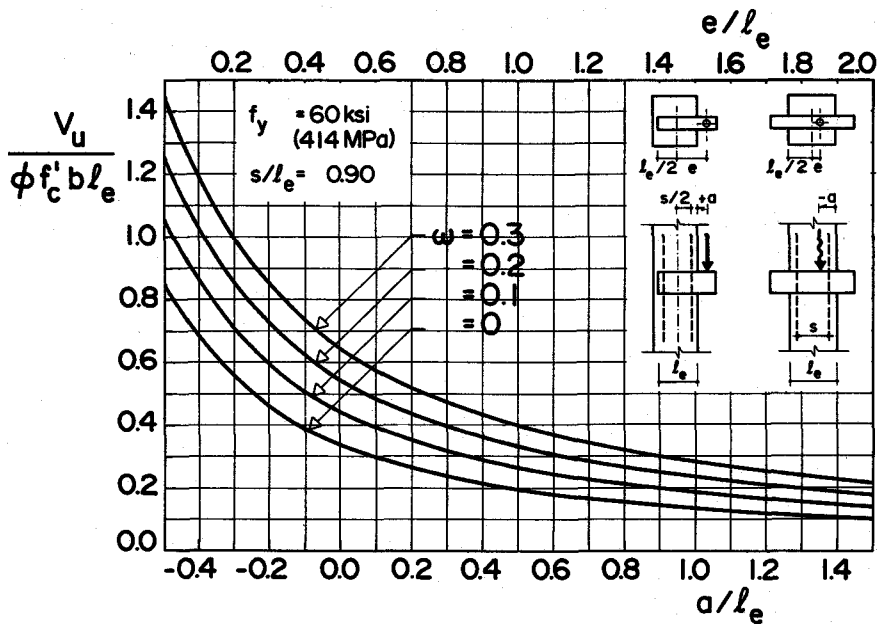


Fig. 12d. Design chart for evaluating parameters ($f_y = 60 \text{ ksi}$, $s/l_e = 0.90$).

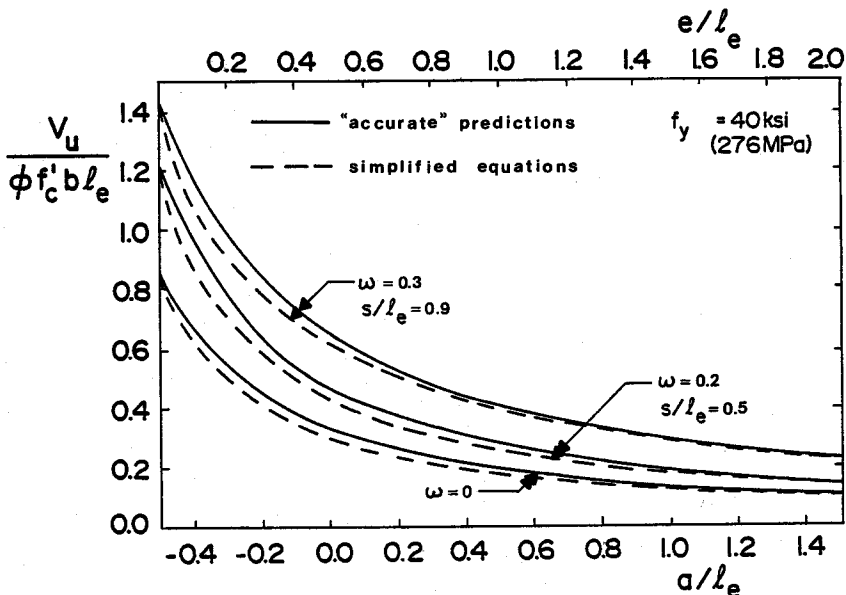


Fig. 13. Comparison of simplified design equations with more accurate predictions.

expressions have been developed taking into account the important variables listed above. The nominal shear capacity of a connection without additional reinforcement can be expressed as:

$$V_c = \frac{0.85 f'_c b l_e}{1 + 3.6 e/l_e} \quad (13)$$

The additional nominal shear capacity provided by welded reinforcement can be expressed as:

$$V_r = \frac{2\omega f'_c b l_e}{1 + \frac{6 e/l_e}{4.8 s/l_e - 1}} \quad (14)$$

The nominal shear capacity of a connection with welded reinforcement can then be found by summing the shear capacity without additional reinforcement with the additional shear capacity provided by welded reinforcement (i.e., $V_n = V_c + V_r$). Fig. 13 compares the predictions of the nominal shear capacity using the

simplified design expressions [Eqs. (13) and (14)] with the predictions from the analysis reported in this paper. As can be seen, the simplified expressions provide a fairly accurate but conservative fit to the more accurate relationships over a wide range of variables.

The embedded steel member must be designed to resist the maximum shear and the maximum moment acting on the member. The maximum shear occurs at the column face while the maximum moment occurs a distance $V_u/(0.85 f'_c b)$ inside the column face, where V_u is the applied load on the embedded member.

Thus, the moment to be resisted by the embedded structural member is:

$$V_u a + \frac{1}{2} V_u^2 / (0.85 f'_c b)$$

A discussion of positioning tolerances for embedded members together with suggestions on the location of load application for design can be found in Reference 3.

Conclusions and Design Recommendations

The analytical model presented in this paper conservatively predicts the capacity of connections incorporating embedded steel members both with and without additional welded reinforcement. The model assumes a linear strain distribution with a maximum strain of 0.003 on the front face of the column or panel. The ACI stress block factors are used to calculate the stress resultant at the front of the connection while a parabolic stress-strain curve is assumed in calculating the stress resultant at the back of the connection. The neutral axis depth is determined such that equilibrium of the forces and the moments on the steel member is achieved. Where welded reinforcement is present in the connection, it is assumed that the strain in the steel is equal in magnitude to the strain in the concrete at the position of the steel.

The experiments indicated that the effective width of the connection extended to the width of the confined column region measured to the outside of the column ties. This effective width, b , is however limited and should not be taken greater than 2.5 times the width of the embedded member, w . Although some tests indicate much larger effective widths, more research is needed before a larger effective width could be justified.

In order to achieve the maximum effective width, closely spaced column ties or other means of confinement must be provided. This reinforcement also controls cracking in the connection region. It is suggested that thin walled hollow structural sections be filled with concrete in order to improve the bearing conditions. In addition, angles can be welded to narrow embedded members in order to increase the effective width.

A series of experiments indicated that the analytical model conservatively predicts the capacity of connections with axial load levels less than 75 percent of the pure axial load capacity of the column. All the specimens tested with low axial loads failed in the concrete and exhibited ductile behavior. For higher levels of axial load a significant decrease in the ductility was observed. If larger ductilities are required, the connection can be designed such that failure takes place in the embedded steel member.

The analytical model has been used to prepare a series of non-dimensionalized design curves for connections with or without additional welded reinforcement. In addition, simplified design expressions are given in Eqs. (13) and (14).

REFERENCES

1. *PCI Design Handbook—Precast and Prestressed Concrete*, First Edition, Prestressed Concrete Institute, Chicago, Illinois, 1971.
2. *PCI Design Handbook—Precast and Prestressed Concrete*, Second Edition, Prestressed Concrete Institute, Chicago, Illinois, 1978.
3. Raths, Charles, H., "Embedded Structural Steel Connections," *PCI JOURNAL*, V. 19, No. 3, May-June 1974, pp. 104-112.
4. *PCI Manual for Structural Design of Architectural Precast Concrete*, Prestressed Concrete Institute, Chicago, Illinois, 1977.
5. Marcakis, K., "Precast Concrete Connections with Embedded Steel Members," M. Eng. thesis, Department of Civil Engineering and Applied Mechanics, McGill University, March 1979, 124 pp.
6. Clarke, J. L., and Symmons, R. M., "Tests on Embedded Steel Billets for Precast Concrete Beam-Column Connections," Technical Report 42.523, Cement and Concrete Association, Wexham Springs, England, August 1978, 12 pp.

APPENDIX A—DESIGN EXAMPLES

The following two numerical examples illustrate the proposed method for designing precast concrete connections incorporating embedded steel members.

EXAMPLE 1

Data: A 4 x 6 x 3/8 in. (102 x 152 x 10 mm) hollow structural steel section is embedded in a 12 x 10 in. (305 x 254 mm) precast column as shown in Fig. A1. The concrete strength, f'_c , is 4000 psi (27.6 MPa) and the yield stresses of the steel reinforcement and the hollow structural section are 60 and 36 ksi (414 and 248 MPa), respectively.

Required: Design the connection to carry an ultimate design shear of 65 kips (289 kN) located 4 in. (102 mm) from the column face.

Solution:

- (a) Determine the effective width, b , of the connection

The width to the outside of the column ties = 7.0 in. The width, b shall not be greater than $2.5w = 2.5 \times 4 = 10$ in. Therefore, use $b = 7.0$ in. (229 mm).

- (b) Compute a/l_e ratio and determine if welded reinforcement is required

$$a/l_e = 4/10 = 0.40$$

$$\frac{V_u}{\phi f'_c b l_e} = \frac{65}{0.85 \times 4 \times 7 \times 10} = 0.273$$

From the design charts it is evident that welded reinforcement is necessary (i.e., ω is greater than zero) for this shear and eccentricity of loading.

- (c) Choice of welded reinforcement

Assume that the welded reinforcement is placed 2.25 in. (57 mm) from

the front face of the column and 1 in. (25 mm) from the back of the embedded member. Since the reinforcement is not symmetrically placed calculate the spacing, s , such that $s/2$ equals the distance from the center of embedment to the closer reinforcement (the front reinforcement in this case).

Therefore, $s/2 = l_e/2 - 2.25$ in. and thus $s = 5.5$ in. giving:

$$s/l_e = 5.5/10 = 0.55$$

Interpolating between the design curves in Figs. 12c and 12d gives a required ω equal to 0.15. The required area of welded reinforcement is therefore:

$$\begin{aligned} A_s &= A'_s = \omega b l_e (f'_c / f_y) \\ &= 0.15 \times 7.0 \times 10.0 \times 4.0/60 \\ &= 0.70 \text{ in.}^2 \text{ (452 mm}^2\text{)} \end{aligned}$$

A reinforcing bar welded to the embedded member as shown in Fig. A1 will develop a tensile force at one end and a compressive force at the other end of the bar. Therefore, the effective area of each bar is twice the cross-sectional area of the bar as long as the appropriate development lengths are provided. Choose 2—#4 bars at the front and at the back of the connection with an effective area of:

$$\begin{aligned} A_s &= A'_s = 4 \times 0.20 = 0.80 \text{ in.}^2 \\ &\quad (516 \text{ mm}^2) \end{aligned}$$

The reinforcing bars are welded to the embedded member with a 4 in. (102 mm) weld on each side of the bar.

- (d) Capacity of steel section

$$\begin{aligned} M_u &= V_u a + \frac{1}{2} V_u^2 / (0.85 f'_c b) \\ &= 65 \times 4 + \frac{1}{2} \times 65^2 / (0.85 \times 4 \times 7) \\ &= 348.8 \text{ in.-kips (39.4 kN-m)} \end{aligned}$$

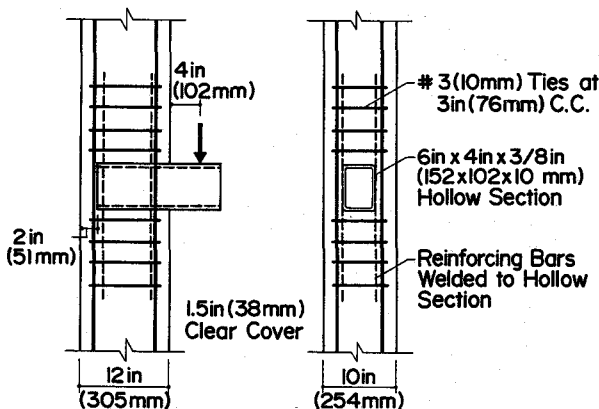


Fig. A1. Design Example 1.

$$\begin{aligned} \text{Steel Stress} &= \frac{M_u}{\phi Z_s} \\ &= \frac{348.8}{0.9 \times 13.61} \\ &= 28.5 \text{ ksi} \\ &= 196.3 \text{ MPa} \end{aligned}$$

The shear design capacity is:

$$\begin{aligned} \phi V_n &= \phi (0.55 f_y h t) \\ &= 0.90 \times 0.55 \times 36 \times 2 \times 6 \times \\ &\quad 0.375 \\ &= 80.2 \text{ kips (357 kN)} \end{aligned}$$

Therefore, the steel section is adequate.

The steel section will be filled with concrete over the embedment length to ensure uniform bearing of the embedded member.

(e) Design using the simplified expressions for V_c and V_r

$$\begin{aligned} V_n &= V_u / \phi = 65 / 0.85 = 76.47 \text{ kips} \\ &\quad (340 \text{ kN}) \\ e/l_e &= 9/10 = 0.90 \end{aligned}$$

The concrete capacity can be found from Eq. (13):

$$\begin{aligned} V_c &= \frac{0.85 f'_c b l_e}{1 + 3.6 e/l_e} \\ &= \frac{0.85 \times 4 \times 7 \times 10}{1 + 3.6 \times 0.9} \\ &= 56.13 \text{ kips (250 kN)} \end{aligned}$$

Therefore, the required welded reinforcement capacity is:

$$\begin{aligned} V_r &= 76.47 - 56.13 = 20.34 \text{ kips} \\ &\quad (90.5 \text{ kN}) \end{aligned}$$

Determine the amount of reinforcement required from Eq. (14):

$$\begin{aligned} \omega_{req} &= \frac{V_r}{2 f'_c b l_e} \left(1 + \frac{6 e/l_e}{4.8 s/l_e - 1} \right) \\ &= \frac{20.34}{2 \times 4 \times 7 \times 10} \times \\ &\quad \left(1 + \frac{6 \times 0.9}{4.8 \times 0.55 - 1} \right) \\ &= 0.156 \end{aligned}$$

Therefore, choose the same welded reinforcement details shown in Part (c) above.

EXAMPLE 2

Data: An interior precast column connection for an industrial structure is shown in Fig. A2. The column is 16 in. (406 mm) square. The concrete strength, f'_c , is 4500 psi (31 MPa) and the yield stress of the embedded steel member is 36 ksi (248 MPa).

Required: Design the connection for the two loading conditions shown in Fig. A2.

Solution:

- (a) Determine required width, w , of embedded member for symmetrical loading condition

For the symmetrical loading case, $e = 0$, therefore:

$$\frac{V_u}{\phi f'_c b l_e} = 0.85$$

Therefore, the required effective width, b , is:

$$b = \frac{440}{0.85 \times 0.85 \times 4.5 \times 16} \\ = 8.46 \text{ in. (215 mm)}$$

The maximum b allowed for this column (to the outside of the column ties) is 13 in. (330 mm) which exceeds the required b .

The minimum w required is:

$$8.46/2.5 = 3.38 \text{ in. (86 mm)}$$

- (b) Determine w required for unsymmetrical loading case

The resultant shear is 330 kips (1468 kN) located 4.0 in. (102 mm) from the center of embedment. Therefore, $e/l_e = 4.0/16.0 = 0.250$.

From Fig. 12c or 12d for the case where $\omega = 0$ (no welded reinforcement):

$$\frac{V_u}{\phi f'_c b l_e} = 0.500$$

Therefore, the required effective width, b , is:

$$b = \frac{330}{0.85 \times 0.50 \times 4.5 \times 16} \\ = 10.78 \text{ in. (274 mm)}$$

The maximum b allowed is 13.0 in.

The minimum w required is:

$$10.78/2.5 = 4.31 \text{ in. (110 mm)}$$

- (c) Determine size and type of embedded member

The required area for shear is:

$$\frac{V_u}{\phi 0.55 f_y} = \frac{220}{0.9 \times 0.55 \times 36} \\ = 12.35 \text{ in.}^2 \text{ (7968 mm}^2\text{)}$$

$$M_u = V_u a + \frac{1}{2} V_u^2 / (0.85 f'_c b) \\ = 220 \times 4 + \frac{1}{2} \times 220^2 / (0.85 \times 4.5 \times 13) \\ = 1367 \text{ in.-kips (154 kN-m)}$$

The required plastic section modulus is:

$$Z_s = \frac{M}{\phi f_y} = \frac{1367}{0.9 \times 36} \\ = 42.2 \text{ in.}^3 \text{ (691392 mm}^3\text{)}$$

Therefore, use a 6 × 6 in. (152 × 152 mm) solid steel bar for the embedded member with an area of shear of 36 in.² (23226 mm²) and a plastic section modulus of 54.0 in.³ (884900 mm³). Alternatively, a smaller width of embedded member could have been selected if welded reinforcement were used.

- (d) Design using the simplified expression for V_c

The calculations for the symmetrical

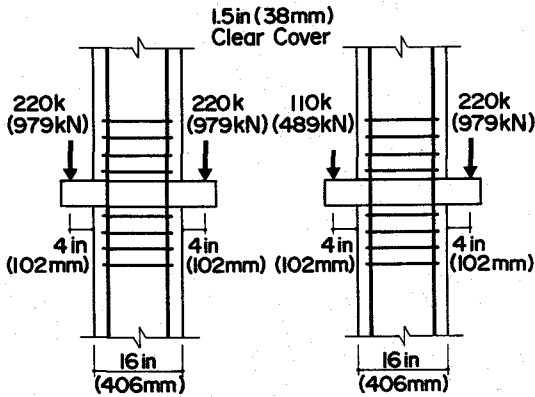


Fig. A2. Design Example 2.

loading case are the same as in Part (a) above.

For the unsymmetrical loading case for $e/l_e = 0.25$ and without additional welded reinforcement then Eq. (13) gives:

$$\begin{aligned} \frac{V_c}{f'_c b l_e} &= \frac{0.85}{1 + 3.6 e/l_e} \\ &= \frac{0.85}{1 + 3.6 \times 0.25} \\ &= 0.447 \end{aligned}$$

Therefore, the required effective width, b , can be determined:

$$\begin{aligned} b &= \frac{330}{0.85 \times 4.5 \times 16 \times 0.447} \\ &= 12.1 \text{ in. (306 mm)} \end{aligned}$$

The minimum w required is:

$$12.1/2.5 = 4.84 \text{ in. (123 mm)}$$

Therefore, choose the same embedded steel member as calculated in Part (c) above.

Acknowledgments

The experimental work was carried out in the Jamieson Structures Laboratory of the Department of Civil Engineering and Applied Mechanics at McGill University. The research reported in this paper was funded by the Natural Sciences and Engineering Research Council of Canada, which is gratefully acknowledged.

Thanks are also extended to Tony Likos and Nadia Townsend for carrying out the embedded plate tests in an undergraduate project.

* * *

NOTE: A Notation section is given on the following page.

APPENDIX B—NOTATION

<p>a = distance from front face of connection to resultant of vertical loads</p> <p>A'_s = area of additional welded reinforcement at rear of embedded member</p> <p>A_s = area of additional welded reinforcement at front of connection</p> <p>b = effective width of section</p> <p>d_b = distance from front face to center of reinforcement near back</p> <p>d_f = distance from front face to center of reinforcement near front</p> <p>C_b = resultant compressive force at back of connection</p> <p>C_f = resultant compressive force at front of connection</p> <p>e = eccentricity of resultant of vertical loads from center of embedment</p> <p>E_s = modulus of elasticity of steel</p> <p>f'_c = compressive strength of concrete</p> <p>f_c = stress in concrete</p> <p>f'_s = stress in additional reinforcement at back of embedded member</p> <p>f_s = stress in additional reinforcement at front of connection</p> <p>f_y = yield stress of steel</p> <p>h = overall depth of embedded member</p> <p>l_e = embedment length</p> <p>M = design moment on embedded member</p> <p>s = distance between symmetri-</p>	<p>cally placed A_s and A'_s</p> <p>t = effective width of embedded member in shear</p> <p>w = width of embedded steel member</p> <p>x_b = distance from back of embedded member to neutral axis</p> <p>x_f = distance from front of connection to neutral axis</p> <p>P = axial load acting on column</p> <p>P_o = pure axial capacity of column</p> <p>V_c = nominal shear capacity of connection without additional reinforcement</p> <p>V_{exp} = experimentally measured shear capacity</p> <p>V_n = nominal shear capacity of a connection</p> <p>V_r = additional nominal shear capacity provided by welded reinforcement</p> <p>V_u = design shear</p> <p>Z_s = plastic section modulus of embedded member</p> <p>α, β = factors defining the equivalent rectangular stress distribution</p> <p>β_1 = ACI stress block factor</p> <p>ϵ_b = maximum strain in concrete at back of embedded member</p> <p>ϵ_c = concrete strain</p> <p>ϵ_f = maximum strain in concrete at front face of connection</p> <p>ϵ_o = strain in concrete at peak compressive stress</p> <p>ϕ = strength reduction factor</p> <p>ω = reinforcement index for additional reinforcement welded to embedded member</p>
---	--

* * *

Discussion of this paper is invited.
Please forward your comments to
PCI Headquarters by March 1, 1981.